

Effect of Mn substitution on superconductivity in iron selenide (Li, Fe)OHFeSe single crystals

Yiyuan Mao(毛义元), Zian Li(李子安), Huaxue Zhou(周花雪), Mingwei Ma(马明伟), Ke Chai(柴可), Shunli Ni(倪顺利), Shaobo Liu(刘少博), Jinpeng Tian(田金鹏), Yulong Huang(黄裕龙), Jie Yuan(袁洁), Fang Zhou(周放), Jianqi Li(李建奇), Kui Jin(金魁), Xiaoli Dong(董晓莉), Zhongxian Zhao(赵忠贤)

Citation: Chin. Phys. B . 2018, 27(7): 077405. **doi:** 10.1088/1674-1056/27/7/077405

Journal homepage: http://cpb.iphy.ac.cn; http://iopscience.iop.org/cpb

What follows is a list of articles you may be interested in

Doping Mn into $(Li_{1-x}Fe_x)OHFe_{1-y}Se$ superconducting crystals via ion-exchange and ion-release/introduction syntheses

Huaxue Zhou(周花雪), Shunli Ni(倪顺利), Jie Yuan(袁洁), Jun Li(李军), Zhongpei Feng(冯中沛), Xingyu Jiang(江星宇), Yulong Huang(黄裕龙), Shaobo Liu(刘少博), Yiyuan Mao(毛义元), Fang Zhou(周放), Kui Jin(金魁), Xiaoli Dong(董晓莉), Zhongxian Zhao(赵忠贤)

Chin. Phys. B . 2017, 26(5): 057402. **doi:** 10.1088/1674-1056/26/5/057402

Controlled synthesis of ferromagnetic $MnSe_x$ particles

Junjie Sun(孙俊杰), Chao Li(李超), Duo Chen(陈铎), Shishou Kang(康仕寿), Guolei Liu(刘国磊), Shuyun Yu(于淑云), Guangbing Han(韩广兵), Liangmo Mei(梅良模)

Chin. Phys. B . 2016, 25(10): 107405. **doi:** 10.1088/1674-1056/25/10/107405

Hybrid crystals of cuprates and iron-based superconductors

Xia Dai(代霞), Cong-Cong Le(勒聪聪), Xian-Xin Wu(吴贤新), Jiang-Ping Hu(胡江平)

Chin. Phys. B . 2016, 25(7): 077402. **doi:** 10.1088/1674-1056/25/7/077402

Synthesis of large FeSe superconductor crystals via ion release/introduction and property characterization

Dongna Yuan(苑冬娜), Yulong Huang(黄裕龙), Shunli Ni(倪顺利), Huaxue Zhou(周花雪), Yiyuan Mao(毛义元), Wei Hu(胡卫), Jie Yuan(袁洁), Kui Jin(金魁), Guangming Zhang(张广铭), Xiaoli Dong(董晓莉), Fang Zhou(周放)

Chin. Phys. B . 2016, 25(7): 077404. **doi:** 10.1088/1674-1056/25/7/077404

Superconductivity in Sm-doped $CaFe_2As_2$ single crystals

Dong-Yun Chen(陈东云), Bin-Bin Ruan(阮彬彬), Jia Yu(于佳), Qi Guo(郭琦), Xiao-Chuan Wang(王小川), Qing-Ge Mu(穆青隔), Bo-Jin Pan(潘伯津), Tong Liu(刘通), Gen-Fu Chen(陈根富), Zhi-An Ren(任治安)

Chin. Phys. B . 2016, 25(6): 067403. **doi:** 10.1088/1674-1056/25/6/067403

Effect of Mn substitution on superconductivity in iron selenide (Li, Fe)OHFeSe single crystals*

Yiyuan Mao(毛义元)[1,2,†], Zian Li(李子安)[1,2,†], Huaxue Zhou(周花雪)[1], Mingwei Ma(马明伟)[1,2], Ke Chai(柴可)[3], Shunli Ni(倪顺利)[1,2], Shaobo Liu(刘少博)[1,2], Jinpeng Tian(田金鹏)[1,2], Yulong Huang(黄裕龙)[1,2], Jie Yuan(袁洁)[1], Fang Zhou(周放)[1,2], Jianqi Li(李建奇)[1,2], Kui Jin(金魁)[1,2], Xiaoli Dong(董晓莉)[1,2,‡], and Zhongxian Zhao(赵忠贤)[1,2,§]

[1] *Beijing National Laboratory for Condensed Matter Physics and Institute of Physics, Chinese Academy of Science, Beijing* 100190, *China*
[2] *University of Chinese Academy of Sciences, Beijing* 100049, *China*
[3] *School of Physic, Beijing Institute of Technology, Beijing* 100081, *China*

(Received 11 May 2018; revised manuscript received 15 May 2018; published online 25 June 2018)

We synthesize a series of Mn substituted (Li, Fe)OHFeSe superconductor single crystals via a modified ion-exchange method, with the Mn concentration z (the atomic ratio of Mn:Se) ranging from 0 to 0.07. The distribution homogeneity of the Mn element incorporated into the lattice of (Li, Fe)OHFeSe is checked by combined measurements of high-angle-annular-dark-field (HAADF) imaging and electron energy-loss spectroscopy (EELS). Interestingly, we find that the superconducting transition temperature T_c and unit cell parameter c of the Mn-doped (Li, Fe)OHFeSe samples display similar V-shaped evolutions with the increasing dopant concentration z. We propose that, with increasing doping level, the Mn dopant first occupies the tetrahedral sites in the (Li, Fe)OH layers before starting to substitute the Fe element in the superconducting FeSe layers, which accounts for the V-shaped change in cell parameter c. The observed positive correlation between the T_c and lattice parameter c, regardless of the Mn doping level z, indicates that a larger interlayer separation, or a weaker interlayer coupling, is essential for the high-T_c superconductivity in (Li, Fe)OHFeSe. This agrees with our previous observations on powder, single crystal, and film samples of (Li, Fe)OHFeSe superconductors.

Keywords: FeSe-based superconductors, Mn doping effect, correlation between superconductivity and interlayer separation

PACS: 74.70.Xa, 82.30.Hk, 74.25.–q **DOI:** 10.1088/1674-1056/27/7/077405

1. Introduction

The recently discovered iron selenide (Li, Fe)OHFeSe (FeSe-11111) superconductor[1] has the layered structure formed by a stacking of one superconducting (SC) FeSe layer alternating with one (Li, Fe)OH layer along the c axis. In contrast to the prototypal bulk FeSe ($T_c \sim 9$ K) and intercalated FeSe-122 superconductors like $K_yFe_{2-x}Se_2$ ($T_c \sim 30$ K), the (Li, Fe)OHFeSe intercalate is free from the complications of chemical phase separation and structural transition. Moreover, it shows a high T_c over 40 K (SC phase I), even above 50 K (SC phase II) under a 12.5 GPa pressure,[2] and a Fermi topology similar to the high-T_c (> 65 K) monolayer film of FeSe.[3,4] Therefore, the (Li, Fe)OHFeSe system turns out to be an ideal platform for studying the intrinsic electronic property and high-T_c superconductivity in the iron-based family. Most recently, we uncovered the occurrence of intrinsic electronic phase separation in (Li, Fe)OHFeSe,[5] similar to that in high-T_c cuprate and iron arsenide superconductors, and established a complete electronic phase diagram for (Li, Fe)OHFeSe. In an earlier work,[6] we successfully synthesized Mn substituted (Li, Fe)OHFeSe single crystals, with the doping level z (the atomic ratio of Mn:Se) ~ 0.08 and 0.16. We found that, at this doping range, the superconducting transition temperature remains almost unchanged, with a T_c (~ 40 K) close to the optimal one for the SC phase I. However, how the Mn substitution at lower concentrations would affect the superconductivity of (Li, Fe)OHFeSe is unclear so far.

In this work, we synthesize a series of lightly Mn-substituted (Li, Fe)OHFeSe single crystals via a modified ion-exchange method, with the doping level z ranging from 0 to 0.07. The homogeneity of Mn distribution in the lattice of (Li, Fe)OHFeSe is checked by combined experiments of high-angle-annular-dark-field (HAADF) atomic lattice imaging and electron energy-loss spectroscopy (EELS). Interestingly, we find that the SC transition temperature T_c and unit cell parameter c of the Mn-doped (Li, Fe)OHFeSe samples show parallel V-shaped evolutions with the increasing dopant concentration z. It appears that, with increasing doping level, the Mn dopant first occupies the tetrahedral sites in the (Li, Fe)OH layers before starting to substitute the Fe element in the FeSe

*Project supported by the National Key Research and Development Program of China (Grant Nos. 2017YFA0303003 and 2016YFA0300300), the National Natural Science Foundation of China (Grant No. 11574370), and the Strategic Priority Research Program and Key Research Program of Frontier Sciences of the Chinese Academy of Sciences (Grant Nos. QYZDY-SSW-SLH001, QYZDY-SSW-SLH008, and XDB07020100).

†These authors contributed equally to this work.
‡Corresponding author. E-mail: dong@iphy.ac.cn
§Corresponding author. E-mail: zhxzhao@iphy.ac.cn

© 2018 Chinese Physical Society and IOP Publishing Ltd

layers, leading to the observed V-shaped change in the cell parameter c. A common positive correlation between the SC transition temperature T_c and lattice parameter c is also observed among the present Mn-doped (Li, Fe)OHFeSe samples, regardless of the Mn substitution concentration z. Such a positive correlation has been reported previously for powder,[7] single crystal,[5,8] and thin film[9,10] samples of Mn-free (Li, Fe)OHFeSe. Therefore, our results indicate that a larger interlayer separation, or a weaker interlayer coupling, is essential for the high-T_c superconductivity in (Li, Fe)OHFeSe. Actually, our previous study[8] has shown that high-T_c (Li, Fe)OHFeSe exhibits a strong electronic two-dimensionality.

2. Experimental details

The x-ray diffraction (XRD) measurements were performed at room temperature on an 18 kW MXP18 A-HF diffractometer with Cu-K_α radiation, using a 2θ range from 5° to 80° and a 2θ scanning step of 0.01° (single crystal) or 0.02° (powder). The average chemical stoichiometry of Fe, Se, and Mn for the single crystal samples was determined by inductively coupled plasma atomic emission spectrometry (ICP-AES). The in-plane electrical resistivity was measured on a Quantum Design PPMS-9. The dc magnetic measurements were carried out on a SQUID magnetometer (Quantum Design MPMS XL-1). The EELS technique combined with a transmission electron microscope (TEM) was used for probing the local composition and spectroscopic information of the specimens. A JEM ARM200F 80–200 TEM (JEOL, Inc.) operated at 200 kV was used for EELS and atom-column-resolved scanning transmission electron microscopy (STEM) HAADF imaging. The microscope is equipped with both probe and image aberration correctors (CEOS GmbH). The electron energy-loss (EEL) spectra were acquired in STEM mode using a $\sim$ 1 nm electron probe with an energy resolution of $\sim$ 0.6 eV or better, as evaluated from the full-width at half-maximum of the zero-loss peak. The 1 nm probe size in STEM mode was intentionally broadened to minimize the electron beam damage on the sample, with parameters for high EELS signal and energy resolution rather than maximum spatial resolution. The spectra were recorded using a dispersion of 0.3 eV/channel and acquisition time of 0.5 s for each spectrum image to minimize electron irradiation damage. The convergence and collection semi-angles were estimated to be 20 mrad and 26.5 mrad, respectively.

The Mn-doped and Mn-free (Li, Fe)OHFeSe single crystals were synthesized via a modified ion-exchange method that we developed and first reported elsewhere.[6,8] The raw materials were 0.003 mol selenourea (Alfa Aesar, 99% purity), 4 g LiOH·H_2O (Alfa Aesar, 98% purity), 0.00375 mol mixture of Fe (Alfa Aesar, 99.998% purity) and Mn (Alfa Aesar, 99.95% purity) powders. All the starting materials were mixed with 5 mL de-ionized water and a piece of $K_2Fe_4Se_5$ single crystal, before being loaded into an autoclave. The autoclave was heated at 120 °C for 72 h and cooled to 50 °C at a rate of 0.5 °C/h. The as-grown Mn-doped and Mn-free (Li, Fe)OHFeSe single crystals were washed by de-ionized water for several times.

3. Results and discussion

Figure 1 displays the XRD patterns for all the Mn-doped and Mn-free (Li, Fe)OHFeSe single crystal samples. Six Mn-doped samples denoted by Mε, M1, M2, M4, M6, M7 have the Mn concentrations of $z \sim \varepsilon$, 0.01, 0.02, 0.04, 0.06, and 0.07, respectively. Here ε means a slight quantity of the doped Mn that is undetectable by ICP-AES. Two Mn-free samples are named as S41 and S40, with the numbers standing for the T_c values. All the Mn-free and Mn-doped (Li, Fe)OHFeSe samples exhibit a single preferred crystal orientation of (001) (Fig. 1(a)). The powder XRD patterns of the single crystal samples are given in Fig. 1(b). All the reflections in each powder XRD pattern can be well indexed on the known tetragonal structure (space group $P4/nmm$) for (Li, Fe)OHFeSe. No impurity phases can be detected by the powder XRD. The calculated lattice parameters a and c are listed in Table 1.

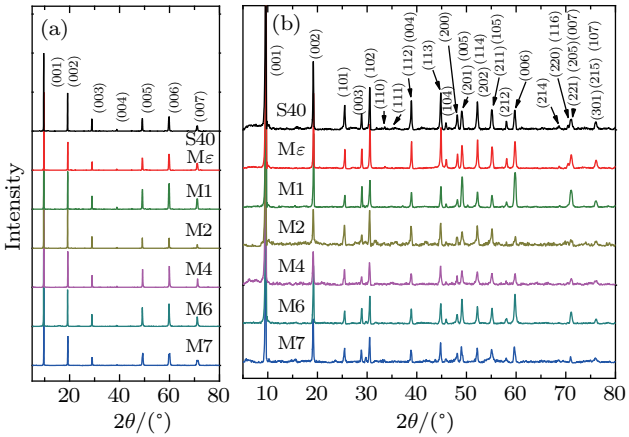


Fig. 1. (color online) (a) XRD spectra for single crystal flakes of the Mn-free and Mn-doped (Li, Fe)OHFeSe, all showing a single preferred crystal orientation of (001). (b) Powder XRD patterns for the single crystal samples.

Table 1. The superconducting transition temperature, unit cell parameters, and chemical composition for Mn-free and Mn-doped (Li, Fe)OHFeSe samples.

Sample	T_c/K	a/Å	c/Å	Fe:Se	z (Mn:Se)
S40	40.4	3.78264(7)	9.2918(2)	1.20	
Mε	38.6	3.7825(3)	9.2915(7)	1.19	ε^*
M1	37.1	3.7835(2)	9.2884(4)	1.14	0.01
M2	36.5	3.7836(2)	9.2696(2)	1.22	0.02
M4	37.8	3.7836(2)	9.2797(3)	1.20	0.04
M6	39.0	3.7869(3)	9.2901(5)	1.18	0.06
M7	40.9	3.7801(2)	9.2961(3)	1.14	0.07

*Here ε means a slight quantity of the doped Mn that is undetectable by ICP-AES.

The homogeneity of Mn distribution in the structure of (Li, Fe)OHFeSe is checked by HAADF atomic lattice imag-

ing. In the HAADF imaging, the recorded contrast arises primarily from Rutherford and thermal diffuse scattering. Under our experimental conditions, the HAADF intensity scales to a good approximation with the atomic number $Z^{1.7}$ and the specimen thickness, as the selected area of interest is sufficiently thin. Figure 2(a) shows an atomically resolved HAADF image of the edge of a typical Mn-doped (Li, Fe)OHFeSe thin flake that is oriented along the [001] crystallographic zone-axis relative to the incident electron beam. Along the [001] zone-axis, a typical square lattice (projected *a*–*b* plane in Fig. 2(a)) is recognized with the bright spots corresponding to the Se/O columns, as indicated in the schematics of the unit cell model. It is noteworthy that due to their relative small atomic numbers compared with the Se element, the Fe columns in the FeSe layers or in the (Li, Fe)OH layers are very weakly visible, as denoted by a white arrow. For the same reasoning, no discernible contrasts can be associated with the Mn dopant, as the Mn substitution is very low in the present samples. Nevertheless, these atomic images measured from tens of flakes do not show any lattice anomalies that could result from Mn (or Mn oxides) impurity phases or precipitates.

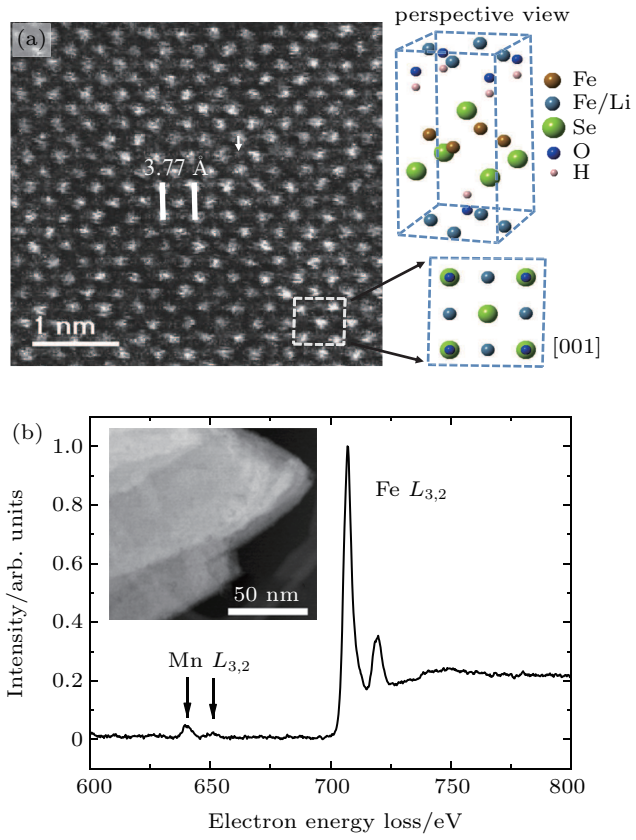


Fig. 2. (color online) HAADF imaging and EELS for typical Mn-doped (Li, Fe)OHFeSe samples. (a) HAADF image of a sample thin flake recorded along [001] crystallographic zone-axis with schematic atomic models. (b) Typical background-subtracted EEL spectrum obtained from an area of 5 nm×5 nm in an EELS–STEM mode, displaying the characteristic $L_{3,2}$-edges for Mn and Fe. The inset shows a low magnification HAADF image of the specimen area for EELS–STEM measurements.

The EEL spectra were simultaneously recorded with relative low-magnification HAADF images in the STEM mode. The characteristic energy of core loss edges in EELS, resulting from inner-shell ionization, provides direct spectroscopic information about the samples. The usefulness of STEM–EELS techniques has been demonstrated in the previous work on iron arsenide superconductors. In the present study, we combine STEM and EELS to probe the local chemical information of the Mn/Fe sites, especially the substitution homogeneity. Figure 2(b) shows a typical background-subtracted EEL spectrum recorded from an area of about 5 nm×5 nm, the selected area scanned across by a ∼ 1-nm-sized electron beam, from which the presence of $L_{3,2}$ edges for Mn and Fe is clearly observed. The inset in Fig. 2(b) shows a low-magnification HAADF image of the specimen area used for STEM–EELS measurement. Such measurements were carried out for tens of different regions to check the homogeneity of Mn substitution. The resultant EEL spectra are similar to that in Fig. 2(b), within experimental errors, but with slight variations in the peak magnitudes in the Mn *L*-edges. However, due to the small Mn concentration and the general difficulties of compositional quantification by EELS, this study cannot yield the exact value of the Mn/Fe atomic ratio.

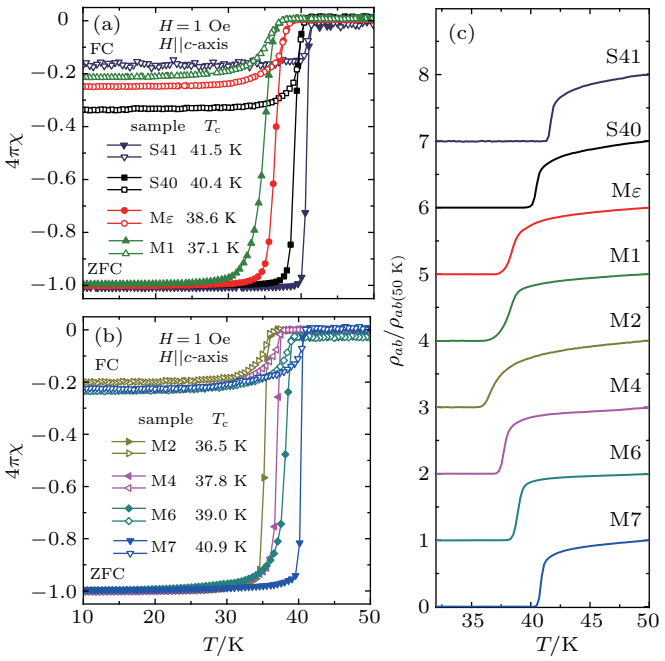


Fig. 3. (color online) (a) and (b) The temperature dependence of the static magnetic susceptibility for the Mn-free and Mn-doped (Li, Fe)OHFeSe samples. A magnetic field of 1 Oe is applied along the *c*-axis. The magnetic susceptibilities are corrected for demagnetization factor. (c) The temperature dependence of reduced in-plane electrical resistivity near the superconducting transition. All the samples show the zero resistivity.

Both the HAADF atomic lattice imaging and STEM–EELS measurements of the Mn-doped (Li, Fe)OHFeSe samples indicate that the employed ion-exchange hydrothermal

syntheses have successfully incorporated the Mn element into the (Li, Fe)OHFeSe lattice. However, quantification of the doped Mn and locally pinpointing the lattice sites at which the Mn dopant locates (in the FeSe or (Li, Fe)OH layers) remain unsolved in the present experiments, in part due to the difficulties in obtaining thin specimens oriented along the [100]-type zone-axis. Future studies may address the exact nature of Mn substitution and provide microstructural and compositional correlations with the superconductivity in Mn-doped (Li, Fe)OHFeSe.

The superconductivity of the single crystal samples is characterized by magnetic susceptibility (Figs. 3(a) and 3(b)) and confirmed by in-plane electrical resistivity (Fig. 3(c)) measurements. The superconducting transition temperature T_c is determined by the onset temperature of the diamagnetic transition, and listed in Table 1. All the samples exhibit a sharp superconducting transition and 100% superconducting shielding.

In Fig. 4(a), we plot the T_c and lattice parameter c versus the Mn doping level z by using the data in Table 1. Interestingly, we find that the curves of T_c and c display parallel V-shaped dependences on the substitution concentration z. The lattice parameter c first decreases then increases with the Mn concentration z, showing the minimum at $z \sim 0.02$. There are two distinct tetrahedral sites in the (Li, Fe)OH and FeSe layers, respectively, that may accommodate the Mn dopant. However, the estimated size of the tetrahedral Li/Fe sites (~ 0.77 Å) in the (Li, Fe)OH layers is bigger than that of the tetrahedral Fe sites (close to ~ 0.56 Å) in the FeSe layers, based on the corresponding Li/Fe–O (~ 2.01 Å) and Fe–Se (~ 2.40 Å) bond lengths[1,8,11–13] as well as the ionic radii[14] for O^{2-} (1.24 Å) and Se^{2-} (close to 1.84 Å). The Mn dopant may exhibit an ionic radius intermediate between the sizes of the two distinct tetrahedral sites with the respective ligands of O^{2-} and Se^{2-}. We speculate that, at slight doping levels of $z <\sim 0.02$, the Mn element is incorporated basically into the (Li, Fe)OH layers and it starts to substitute the Fe element in the FeSe layers when the Mn concentration z is further increased up to ~ 0.07. This can account for the observed V-shaped evolution of the cell parameter c with the doping level z, considering the small variation in the cell parameter a. Our results indicate that the Mn substitution alters mainly the interlayer separation of (Li, Fe)OHFeSe, which acts as a control parameter for the superconducting transition temperature T_c. As shown in Fig. 4(b), the commonly seen positive correlation between the T_c and lattice parameter c also occurs among the present Mn-doped (Li, Fe)OHFeSe samples, regardless of the Mn doping level z. Such a positive correlation has been observed previously in our powder,[7] single crystal,[5,8] and thin film[9,10] samples of Mn-free (Li, Fe)OHFeSe superconductors.

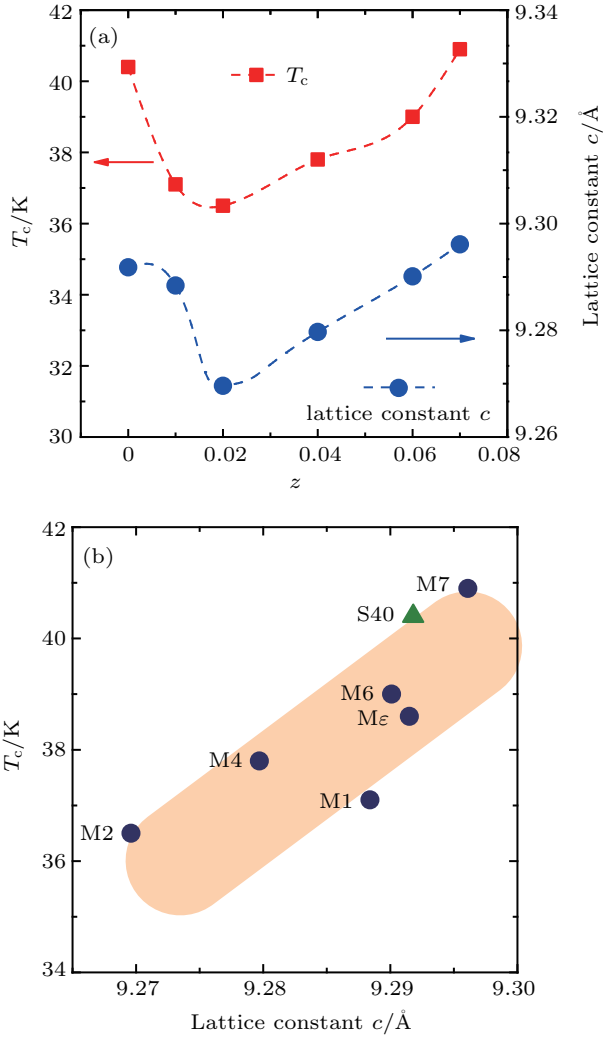


Fig. 4. (color online) (a) Lattice parameter c and superconducting transition temperature T_c as functions of Mn doping level z. The dashed curves are as a guide to the eye. (b) The positive correlation between the SC transition temperature T_c and lattice parameter c among the Mn-doped and Mn-free (Li, Fe)OHFeSe samples, regardless of the Mn doping level z.

4. Conclusion

The modified hydrothermal ion-exchange method manifests itself as an effective technique to dope the Mn element into the layered structure of (Li, Fe)OHFeSe superconductors. The Mn dopant may be accommodated in the tetrahedral sites in the (Li, Fe)OH and FeSe layers depending on the doping level, reducing or enhancing the interlayer separation of (Li, Fe)OHFeSe. A common positive correlation between the superconducting transition temperature T_c and lattice parameter c is also observed among the present Mn-doped (Li, Fe)OHFeSe samples, regardless of the Mn doping level. It is indicated that a larger interlayer separation, or a weaker interlayer coupling, is essential for the high-T_c superconductivity in (Li, Fe)OHFeSe. This is in agreement with the strong electronic two-dimensionality reported previously for the high-T_c (Li, Fe)OHFeSe superconductor.[8]

References

[1] Lu X F, Wang N Z, Wu H, Wu Y P, Zhao D, Zeng X Z, Luo X G, Wu T, Bao W, Zhang G H, Huang F Q, Huang Q Z and Chen X H 2015 *Nat. Mater.* **14** 325

[2] Sun J P, Shahi P, Zhou H X, Huang Y L, Chen K Y, Wang B S, Ni S L, Li N N, Zhang K, Yang W G, Uwatoko Y, Xing G, Sun J, Singh D J, Jin K, Zhou F, Zhang G M, Dong X L, Zhao Z X and Cheng J G 2018 *Nat. Commun.* **9** 380

[3] Niu X H, Peng R, Xu H C, Yan Y J, Jiang J, Xu D F, Yu T L, Song Q, Huang Z C, Wang Y X, Xie B P, Lu X F, Wang N Z, Chen X H, Sun Z and Feng D L 2015 *Phys. Rev. B* **92** 060504(R)

[4] Zhao L, Liang A, Yuan D, Hu Y, Liu D, Huang J, He S, Shen B, Xu Y, Liu X, Yu L, Liu G, Zhou H, Huang Y, Dong X, Zhou F, Liu K, Lu Z, Zhao Z, Chen C, Xu Z and Zhou X J 2016 *Nat. Commun.* **7** 10608

[5] Mao Y, Huan Y, Yuan J, Li Z, Chai K, Ma M, Ni S, Tian J, Liu S, Zhou H, Zhou F, Li J, Zhang G, Jin K, Dong X and Zhao Z 2018 *Chin. Phys. Lett.* **35** 057402

[6] Zhou H, Ni S, Yuan J, Li J, Feng Z, Jiang X, Huang Y, Liu S, Mao Y, Zhou F, Jin K, Dong X and Zhao Z 2017 *Chin. Phys. B* **26** 057402

[7] Dong X, Zhou H, Yang H, Yuan J, Jin K, Zhou F, Yuan D, Wei L, Li J, Wang X, Zhang G and Zhao Z 2015 *J. Am. Chem. Soc.* **137** 66

[8] Dong X, Jin K, Yuan D, Zhou H, Yuan J, Huang Y, Hua W, Sun J, Zheng P, Hu W, Mao Y, Ma M, Zhang G, Zhou F and Zhao Z 2015 *Phys. Re. B* **92** 064515

[9] Huang Y L, Feng Z P, Yuan J, Hu W, Li J, Ni S L, Liu S B, Mao Y Y, Zhou H X, Wang H B, Zhou F, Zhang G M, Jin K, Dong X L and Zhao Z X 2017 arXiv:1711.02920

[10] Huang Y, Feng Z, Ni S, Li J, Hu W, Liu S, Mao Y, Zhou H, Zhou F, Jin K, Wang H, Yuan J, Dong X and Zhao Z 2017 *Chin. Phys. Lett.* **34** 077404

[11] Sun H, Woodruff D N, Cassidy S J, Allcroft G M, Sedlmaier S J, Thompson A L, Bingham P A, Forder S D, Cartenet S, Mary N, Ramos S, Foronda F R, Williams B H, Li X, Blundell S J and Clarke S J 2015 *Inorg. Chem.* **54** 1958

[12] Pachmayr U, Nitsche F, Luetkens H, Kamusella S, Brueckner F, Sarkar R, Klauss H H and Johrendt D 2015 *Angew. Chem.-Int. Ed.* **54** 293

[13] Zhou X, Borg C K H, Lynn J W, Saha S R, Paglione J and Rodriguez E E 2016 *J. Mater. Chem. C* **4** 3934

[14] Shannon R D 1976 *Acta Crystallogr. Sect. A* **32** 751